Effect of Uniaxial Compression on Impurity Conduction in *n*-Type Germanium*

H. FRITZSCHE
Department of Physics and Institute for the Study of Metals, University of Chicago, Chicago, Illinois
(Received October 19, 1961)

Shear strains, which change the donor wave functions, greatly affect impurity conduction, which depends sensitively on the wave-function overlap of neighboring impurity states. Using uniaxial compression along [111], we investigated as a function of stress the critical impurity separation d_c for the transition from nonmetallic to metallic conduction and impurity conduction in the intermediate concentration range, $7\times10^{16}<N<3\times10^{17}$ cm^{-3}. The largest stress applied was 2×10^9 dyne cm^{-2}. The main effect of stress is a change of the activation energy ϵ_2 of impurity conduction. In arsenic- and phosphorus-doped germanium, [111] compression decreases ϵ_2 and increases d_c. In antimony-doped germanium the opposite is observed; compression increases ϵ_2 and decreases d_c. At 1.2°K, [111] compression can increase the resistivity of antimony-doped germanium by a factor of 10^7. Using the same orientation and temperature, a decrease of the resistivity of arsenic-doped germanium by a factor of 5×10^{-4} is observed. These results suggest that (i) the activation energy ϵ_2 depends strongly on the wave function overlap, and (ii) shear strains change the donor wave functions originating from the individual valleys by an amount which is proportional to the valley-orbit splitting of the donor element.

I. INTRODUCTION

SINCE the discovery of impurity conduction by Busch and Labhart[1] in SiC and independently by Hung and Gliessman[2] in Ge, a considerable effort both experimental and theoretical has been devoted[3] to the understanding of this new conduction mechanism. Impurity conduction is due to the fact that a charge carrier has a finite probability for tunneling from an occupied impurity center to a neighboring unoccupied one. In contrast to the normal conduction process at higher temperatures, the carriers are not excited into their respective conduction bands. Mott[4] pointed out, however, that thermal excitation is also necessary for impurity conduction since neighboring impurity centers have in general not the same energy due to Coulomb fields of the compensating minority impurity ions.

It has been found convenient to distinguish three ranges of impurity concentration in which impurity conduction exhibits quite different properties.[5]

The range of low impurity concentrations can be defined by $d/a_H>5$, where d is the average separation of majority impurities and a_H is their effective Bohr radius. In this range impurity conduction exhibits an activation energy which has been named ϵ_3. Theoretical studies[6–8] based on the model of phonon-induced charge tunneling between impurity sites, where a fraction K of the sites is vacant due to compensation, have been quite successful in this range.

In the range of intermediate concentration defined $3<d/a_H<5$ the conduction process is least understood. The resistivity curves exhibit two activation energies ϵ_2 and ϵ_3 at low temperatures and the Hall effect has a complicated temperature dependence.[5,9]

At high impurity concentrations a transition to metallic conduction is observed. Here the conduction process ceases to be thermally activated and the picture of a degenerate semiconductor becomes appropriate.

It is apparent that many factors determine the magnitude and the temperature dependence of impurity conduction. Hence it is important to change only one of the parameters at a time and to study systematically its effect on impurity conduction. With transmutation-doped germanium it was possible[10,11] to study the conduction for fixed compensation K as a function of impurity separation d, and for fixed d as a function of K. These experiments determine the size of the impurity wave functions and the compensation dependence of the activation energy ϵ_3. In the low concentration range the results essentially support the model of impurity conduction as treated by Kasuya and Koide,[6] by Miller and Abrahams,[7] and by Twose.[8]

Since impurity conduction depends sensitively on the overlap of neighboring impurity states, the size and the shape of the impurity wave functions are important parameters in this conduction process. Fortunately, one can change the impurity wave functions considerably by applying elastic shear strains to the semiconductor. This was demonstrated recently[12] by applying uniaxial tension and compression to *n*-type germanium along the [110] crystallographic axis. The anisotropy of the resultant piezoresistance effect agrees well with anisotropy of the strain-modified donor wave

* Work supported by the U. S. Air Force Office of Scientific Research.
[1] G. Busch and H. Labhart, Helv. Phys. Acta **19**, 463 (1946).
[2] C. S. Hung and J. R. Gliessman, Phys. Rev. **79**, 726 (1950).
[3] For references to papers on impurity conduction see references 4 and 5.
[4] N. F. Mott, Can. J. Phys. **34**, 1356 (1956); N. F. Mott and W. D. Twose, *Advances in Physics*, edited by N. F. Mott (Taylor and Francis, Ltd., London, 1961), Vol. 10, p. 107.
[5] H. Fritzsche, J. Phys. Chem. Solids **6**, 69 (1958).
[6] T. Kasuya and S. Koide, J. Phys. Soc. Japan **13**, 1287 (1958).
[7] A. Miller and E. Abrahams, Phys. Rev. **120**, 745 (1960).
[8] W. D. Twose, thesis, Cambridge, 1959 (unpublished).
[9] H. Fritzsche, Phys. Rev. **99**, 406 (1955).
[10] H. Fritzsche and M. Cuevas, Phys. Rev. **119**, 1238 (1960).
[11] H. Fritzsche and M. Cuevas, *Proceedings of the International Conference on Semiconductor Physics, Prague, 1960* (Czechoslovakian Academy of Sciences, Prague, 1961), p. 222.
[12] H. Fritzsche, Phys. Rev. **119**, 1899 (1960).

functions as calculated on the basis of the deformation potential theory.

The fact that we can change the impurity wave functions by means of shear strains enables us to investigate (1) which of the characteristics of impurity conduction depend on the wave-function overlap and their dependence on it, and (2) how the wave functions of the various donor elements change at larger distances from the impurity atom as a function of shear strain.

Regarding the first problem, it is interesting to study the transition from nonmetallic to metallic conduction for various sizes of the ground-state orbit. The possibility of changing the overlap at will may also elucidate the unexplained conduction process in the intermediate impurity concentration range which is associated with the activation energy ϵ_2. It also is important to check whether the activation energy ϵ_3 of impurity conduction in the low-concentration range is independent of the wave-function overlap and only determined by the Coulomb interaction of the charge carriers with the compensating impurity ions as predicted by Mott. Finally, the contribution of the higher lying threefold state of the 1*s* multiplet to impurity conduction in *n*-type germanium can be investigated since large uniaxial compression along [111] yields a simple and almost hydrogenic energy level scheme for the group *V* donors.[13]

In order to study the second problem, i.e., the change of the wave functions themselves, it would be helpful but it is not necessary to have a complete understanding of the impurity conduction process. By comparing the effect of strain on germanium doped with either antimony, arsenic, or phosphorus, which are donors with very different valley-orbit splittings, one can investigate how the breakdown of the effective mass approximation affects the strain-induced changes of the donor wave function. The valley-orbit splittings 4Δ of these donors are $4\Delta(\mathrm{Sb})=0.57\times10^{-3}$ ev,[14] $4\Delta(\mathrm{As})=4.15\times10^{-3}$ ev,[15–17] and $4\Delta(\mathrm{P})=2.9\times10^{-3}$ ev.[16,17]

The object of the present work is to study the effect of uniaxial compression along the [111] direction on impurity conduction in the intermediate concentration range and on the transition from nonmetallic to metallic conduction, and to compare for this stress orientation the piezoresistance effect of antimony-, arsenic-, and phosphorus-doped germanium.

Compression along [111] has been chosen because it yields the largest change of the donor wave function. It depresses one conduction band valley with respect to the remaining three.[13] This yields in the limit of large stresses a pancake-shaped donor wave function[18] which is composed of Bloch functions near the minimum of only the single lowest-lying valley.

TABLE I. Sample characteristics.

Sample	ρ (300°K) (ohm-cm)	R (300°K) (cm³ coul⁻¹)	R (78°K) (cm³ coul⁻¹)	N_D (cm⁻³)	d (A)
Sb-1	0.038	71.2	124	8.76×10^{16}	139.5
Sb-2	0.0318	66.8	105	9.34×10^{16}	136.8
Sb-3	0.0224	40.8	65.6	1.53×10^{17}	116
Sb-4	0.018	29.7	45.7	2.10×10^{17}	104.4
As-1	0.0325	67	113.6	9.32×10^{16}	137
As-2	0.0249	46.7	78.3	1.33×10^{17}	121.5
As-3	0.0196	33.5	55.7	1.86×10^{17}	108.6
As-4	0.0169	25.25	42.3	2.47×10^{17}	98.8
As-5	0.0151	22.1	35.8	2.82×10^{17}	94.55
As-6	0.0126	17.3	26.5	3.61×10^{17}	87.0
P-1	0.0293	58.0	99.0	1.08×10^{17}	130.5
P-2	0.025	46.1	76.8	1.35×10^{17}	120.8
P-3	0.0216	36.8	61.3	1.70×10^{17}	112.1
P-4	0.01735	27.5	47.1	2.26×10^{17}	101.7
P-5	0.0148	21.6	34.1	2.89×10^{17}	93.8

We report measurements at temperatures between 300°K and 1.3°K of the piezoresistance effect of germanium doped with either Sb, As, or P. The compressional stresses employed range from 2×10^7 to 2×10^9 dyne/cm². The resistivity was measured for current flowing parallel to the stress direction.

In a subsequent paper (in the following referred to as II) the strain-modified donor wave functions will be calculated and an attempt will be made to explain the present results.

II. EXPERIMENTAL DETAILS

All germanium samples were cut from single crystals perpendicular to the growth axis to minimize the impurity concentration gradient along their length. The dislocation density was less than 2×10^3 cm^{-2}. The orientation was obtained by x rays to better than one degree. The sizes, surface treatment, and mounting of the samples as well as the cryostat have been described before.[15] For applying compressional stress it was found more convenient to slip the sample into closely fitting nylon cups instead of cementing them into brass cups. The reproducibility of the piezoresistance effect was repeatedly checked and found to be better than 1%.

III. EXPERIMENTAL RESULTS

Table I lists the samples used in this investigation with their Hall coefficient R and resistivity ρ at 300° and 78°K, their donor concentration N_D, and the average donor separation d. The degree of compensation is estimated to be less than 2%. The sample code number indicates the donor element.

[13] P. J. Price, Phys. Rev. **104**, 1223 (1956); see also the discussion by H. Fritzsche, following paper [*ibid.* **125**, 1560 (1962)].
[14] H. Fritzsche, Phys. Rev. **120**, 1120 (1960).
[15] H. Fritzsche, Phys. Rev. **115**, 336 (1959).
[16] G. Weinreich and H. G. White, Bull. Am. Phys. Soc. **5**, 60 (1960).
[17] D. K. Wilson and G. Feher, Bull. Am. Phys. Soc. **5**, 60 (1960).
[18] W. Kohn, in *Solid-State Physics*, edited by F. Seitz and D. Turnbull (Academic Press, Inc., New York, 1957), Vol. 5, p. 257.

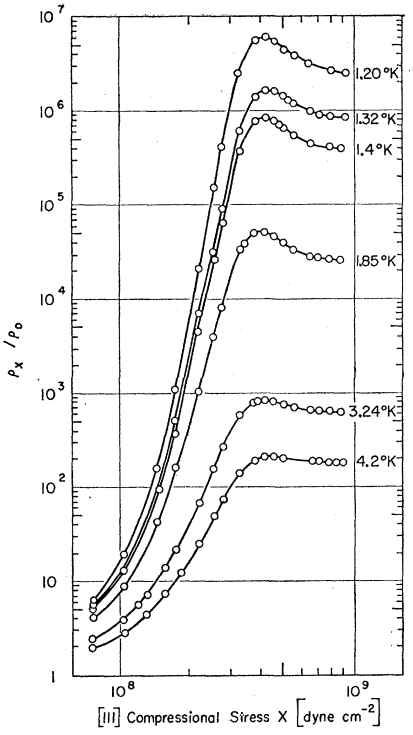

FIG. 1. Sb-doped germanium. Ratio of resistivity with stress to the value without stress of Sb-2 as a function of uniaxial compression in the [111] direction. The temperatures are in the range of impurity conduction.

A. Antimony-Doped Germanium

Figure 1 shows the ratio ρ_X/ρ_0 for Sb-2 as a function of compressional [111] stress for various temperatures in the range of impurity conduction. ρ_X and ρ_0 are the resistivities with and without stress, respectively. ρ_X/ρ_0 increases rapidly, reaches a maximum near 4×10^8 dyne/cm^2, and then drops by a factor of between 1 and 2 before it saturates at about 8×10^8 dynes/cm^2. We observe a strong temperature dependence. Particularly at the lowest temperatures the resistivity changes become very large.

We did expect a large increase in resistivity of impurity conduction because of the following. Compression along [111] lifts the degeneracy of the valleys by shifting the [111] valley down and the remaining three valleys up in energy.[13] Hence the valleys no longer contribute equally to the ground state wave function, but with increasing stress the lower energy valley contributes more and more strongly. The limiting form of the ground-state wave function at large stresses is pancake-shaped with the axis of rotation along [111]. This is the direction along which the resistivity was measured. In the [111] direction the extent of the donor wave function, and therefore the overlap of neighboring donor wave functions, is greatly reduced. For carriers tunneling near the plane perpendicular to [111] the overlap still is close to its zero stress value but these carriers hardly contribute to the current along [111]. Thus a large piezoresistance effect was expected, which saturates at high stresses where the limiting form of the donor wave function is reached.

Unexpected was, however, the strong temperature dependence of ρ_X/ρ_0 seen in Fig. 1. In Fig. 2 the resistivity of Sb-2 is plotted for various stresses against $1/T$. The main effect of stress is a change of activation energy ϵ_2 and a small increase in the intercept of the extrapolated $\log\rho$ vs $1/T$ at low temperatures with the $1/T=0$ axis. This is also evident from Fig. 3 which shows ρ_0 (dotted curves) and the saturation values of ρ_X (solid curves) of the Sb-doped samples as a function of $1/T$.

In order to understand the effect of stress on the activation energy of impurity conduction, we have to discuss in more detail the resistivity of unstressed germanium in this concentration range.

Figure 2 of reference 5 shows ρ_0 of Sb-doped germanium as a function of $1/T$. The temperature dependence of the conductivities σ can be approximated by a sum of three exponential terms:

$$\sigma=C_1\exp(-\epsilon_1/kT)+C_2\exp(-\epsilon_2/kT)+C_3\exp(-\epsilon_3/kT). \quad (1)$$

The first term represents the conduction in the conduction band with the donor ionization energy ϵ_1. In the low concentration range, that is $N_D\leq10^{16}$/cm^3, the low-temperature impurity conduction is described by the third term with the activation energy ϵ_3. In the intermediate concentration range impurity conduction exhibits two activation energies ϵ_2 and ϵ_3. It was found that ϵ_2 decreases rapidly with increasing impurity concentration. Before the conduction becomes metallic there is a concentration range ($6.5\times10^{16}\leq N_D\leq1.3\times10^{17}$

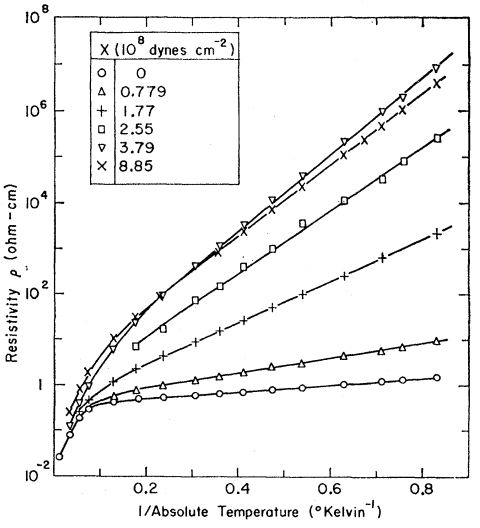

FIG. 2. Sb-doped germanium. Resistivity of Sb-2 for various compressional stresses as a function of $1/T$. The range of impurity conduction extends from about 10°K to the lowest temperatures.

cm^{-3}) in which only one activation energy is found. It was mentioned at that time[5] that this activation energy might be associated with the process which gives rise to the second exponential term in Eq. (2). Some further experimental results, which will be discussed below, suggest that this is the case. Hence we call this activation energy ϵ_2.

The samples Sb-3 and Sb-4 belong to the high concentration range ($N_D > 1.3\times10^{17}$ cm^{-3}). Their resistivity remains constant at low temperatures, which means their conduction is metallic in the sense of Mott.[4] The transition to nonmetallic conduction occurs at a concentration between Sb-3 and Sb-2. The resistivity curves of Sb-1 and Sb-2 exhibit a finite activation energy ϵ_2.

The activation energies ϵ_2 and ϵ_3 measured at zero stress are plotted together with the previously published data against the average impurity separation d in Fig. 4. Up to the critical separation $d_c = 135$ A, $\epsilon_2 = 0$, and the conduction is metallic. For $135\text{ A} < d < 300$ A (transition range) ϵ_2 rises rapidly with increasing d and the activation energy ϵ_3 appears. Beyond about $d = 300$ A, ϵ_3 decreases with increasing d in qualitative agreement with Miller and Abrahams' theory[7] and Mott's model of the interaction of the carriers with the oppositely charged compensating impurity ions. If this Coulomb interaction gives rise to ϵ_3 in the low-concentration range, ϵ_3 is expected to be independent of the amount of overlap.

The origin of the activation energy ϵ_2 observed in the transition range has not yet been explained satisfactorily. We believe that ϵ_2 depends strongly on the wave-function overlap because of the following.

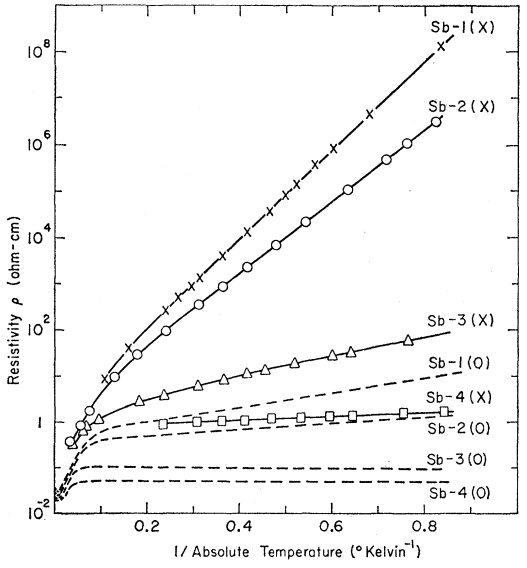

FIG. 3. Resistivity curves of the Sb-doped samples listed in Table I. Dashed curves represent the zero-stress resistivities, solid curves the maximum-stress resistivities measured at $X > 8.8 \times 10^8$ dyne cm^{-2}.

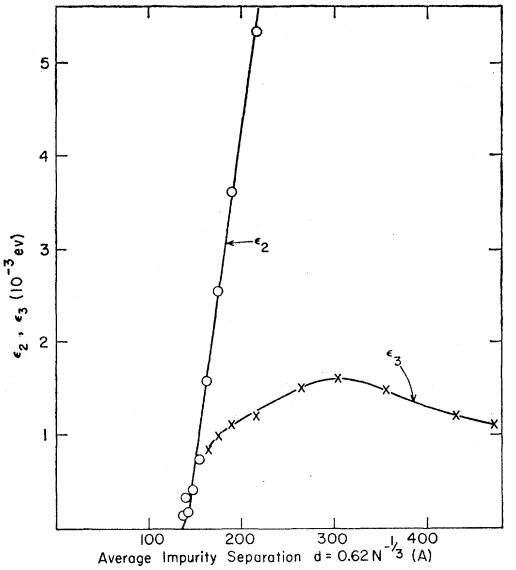

FIG. 4. Sb-doped germanium. Activation energies ϵ_2 and ϵ_3 of impurity conduction [see Eq. (1) of text] as a function of the average impurity separation d.

According to Mott and Twose[4] the transition to metallic conduction occurs at a critical separation $d_c \approx 3.5 a_H$, where a_H is the effective Bohr radius of the impurity. For $d < d_c$ the overlap is so strong that the carriers cease to be localized around individual impurity centers. It is therefore very likely that the sharp drop of ϵ_2 as d approaches d_c in the range $d > d_c$ is caused by the increase in overlap as d is decreased.

This agrees with the results shown in Figs. 2 and 3. The change in ϵ_2 is in the expected direction. The decrease in overlap caused by the compressional [111] stress gives rise to an increase in ϵ_2. Samples Sb-3 and Sb-4 which are metallic at zero stress become nonmetallic and show a finite ϵ_2 at large stress. Sb-1 and Sb-2 show an appreciable increase in ϵ_2 with stress. This accounts for the strong temperature dependence of the piezoresistance effect and for its large magnitude at very low temperatures.

A more quantitative description of this piezoresistance effect can only be attempted when the detailed mechanism of conduction in the transition range is understood. The case of Sb-doped germanium is complicated by the fact that the threefold 1s-like state lies very close to the ground state and probably overlaps it at these high impurity concentrations. In any case the threefold state will contribute strongly to impurity conduction at zero stress. In addition to the effect of the changing overlap of the ground state and the higher-lying states on ϵ_2 the redistribution of carriers over the 1s-like states has to be considered in calculating the piezoresistance effect. Furthermore, the activation energy ϵ_2 will probably depend on a weighted angular average of the wave-function overlap and not only on the overlap in the current direction.

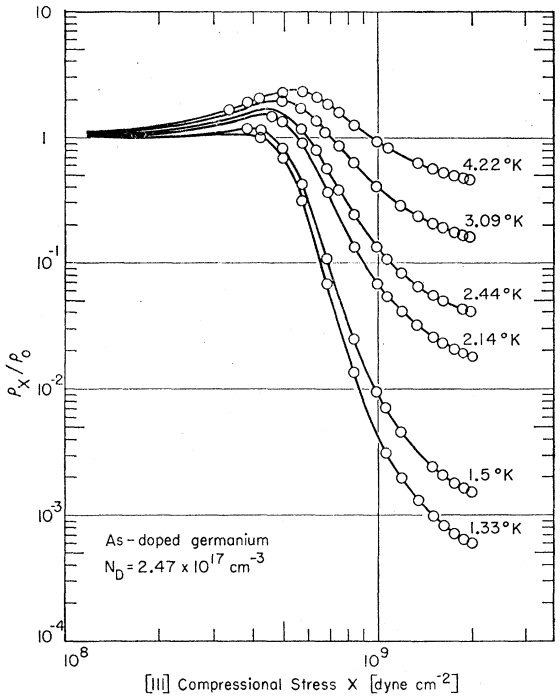

FIG. 5. As-doped germanium. Ratio of resistivity with stress to the value without stress of As-4 as a function of uniaxial compression along the [111] direction. The temperatures are in the range of impurity conduction. Note that saturation has not yet been reached.

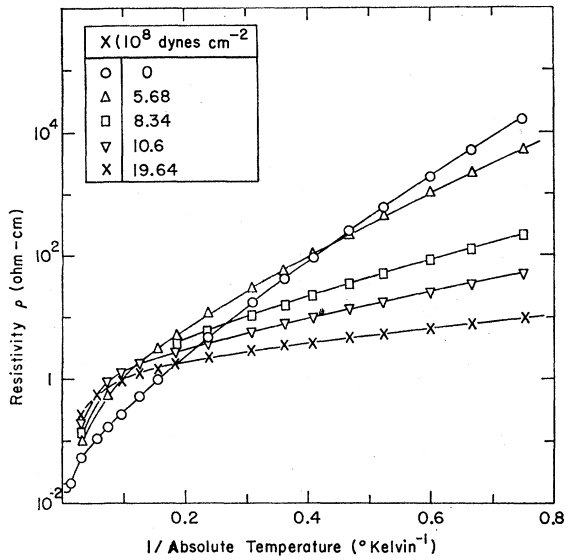

FIG. 6. As-doped germanium. Resistivity of As-4 for various compressional stresses as a function of $1/T$. The range of impurity conduction extends from about 8°K to the lowest temperatures.

B. Arsenic-Doped Germanium

The resistivity ratio ρ_X/ρ_0 of As-4 is plotted against stress in Fig. 5. One observes a striking difference between the piezoresistance of As-doped and of Sb-doped germanium (compare with Fig. 1). The resistivity ratio of As-4 increases only slightly at low stresses and then drops rapidly to very small values. The piezoresistance effect approaches a saturation value at stresses above 2×10^9 d/cm².

That the temperature dependence of ρ_X/ρ_0 is again due to a stress-induced change of the activation energy can be seen in Fig. 6. Here the resistivity of As-4 is plotted against $1/T$ for various values of stress. However, in contrast to the case of Sb donors ϵ_2 of As-doped germanium decreases with increasing stress. This trend is also apparent in Fig. 7 where ρ_0 and the high stress limit of ρ_X of all As-doped samples are plotted against $1/T$. The stress decreases ϵ_2 in all cases. This decrease is accompanied by an increase in the intercept of the extrapolated logρ vs $1/T$ curves at low T with the $1/T=0$ axis. This causes the ρ_0 and ρ_X curves to cross at high temperatures. Sample As-5 almost becomes metallic at large stress.

If the increases of ϵ_2 with decreasing wave-function overlap is a correct assumption then these last results suggest that the wave functions of As donors expand and the overlap increases with compressional stress in contrast to the predicted and observed behavior of Sb donors. That this actually may be the case will be discussed in the subsequent paper II. It will be shown that two opposing effects change the size and the shape of the ground-state wave functions. The removal of the valley degeneracy decreases the overlap as discussed for the case of Sb donors. The other effect is connected with the corrections to the effective mass approximation.

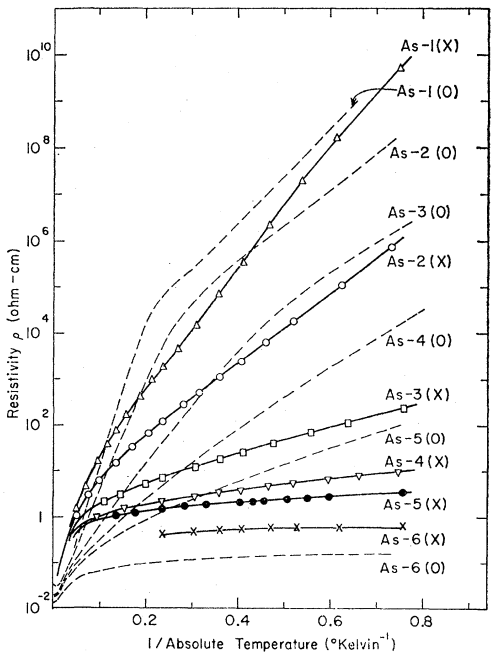

FIG. 7. Resistivity curves of the As-doped samples listed in Table I. Dashed curves represent the zero-stress resistivities, solid curves the resistivities measured at stresses between 1.5×10^9 and 2×10^9 dyne cm^{-2}.

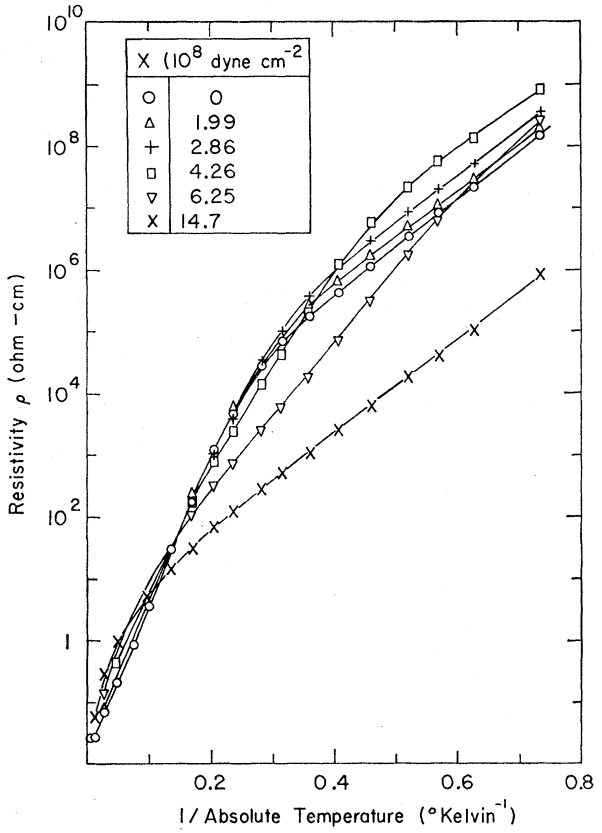

FIG. 8. Resistivity of As-2 for various stresses as a function of $1/T$. The activation energy ϵ_2 is almost unnoticeable at zero stress. It dominates an increasingly larger temperature range at higher stresses.

It increases the wave function and can cause an increase in overlap at large stresses particularly in cases of donors like As which have a large valley-orbit splitting. For Sb donors this second effect plays a negligible role because of their small valley-orbit splitting.

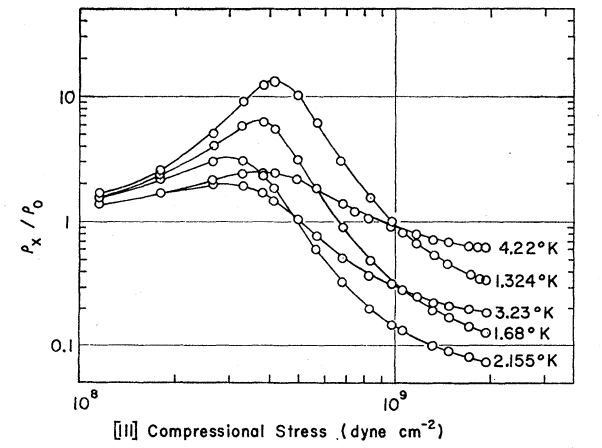

FIG. 9. P-doped germanium. Ratio of resistivity with stress to the value without stress of P-1 as a function of uniaxial compression along [111]. The temperatures below 3°K are in the range of impurity conduction. Note that saturation has not yet been reached for the lowest temperatures.

The ρ_0 curves of As-1, As-2, and As-3 (Fig. 7) exhibit both activation energies ϵ_2 and ϵ_3, where $\epsilon_2 > \epsilon_3$. The onset of the ϵ_3 process shifts to lower temperatures as N_D increases. Because of this and because of the strong concentration dependence of ϵ_2, we assumed that the single activation energy of As-4, 5, and 6 is ϵ_2 rather than ϵ_3. To verify this point we investigated the stress dependence of the ϵ_2 and the ϵ_3 process in the case of As-2. Figure 8 shows that the resistivity associated with ϵ_3 increases with stress, leaving ϵ_3 almost constant. ϵ_2, on the other hand, decreases rapidly. This causes the onset of the process to shift to lower temperatures and to vanish at the higher stresses. We conclude from this that the process, for which the activation energy depends strongly on separation and overlap, predominates in the concentration range below the transition to metallic conduction. The conduction observed in the high-stress limit at these impurity concentrations is also associated with the ϵ_2 process.

Despite the large valley-orbit splitting of As donors, $4\Delta/k \approx 50°\text{K}$, the higher lying threefold state can contribute considerably to the zero- and low-stress impurity conduction because its wave functions extend much further out than the ground-state wave function. This will be shown in (II). The temperature dependence of the contribution of the threefold state may be one of the reasons for the slight temperature dependence of ρ_0 which is observed in addition to the exponential terms of Eq. (1).

C. Phosphorus-Doped Germanium

The valley-orbit splitting of phosphorus lies with $4\Delta = 2.9\times10^{-3}$ ev, between that of antimony (0.57×10^{-3} ev) and of arsenic (4.15×10^{-3} ev). One therefore

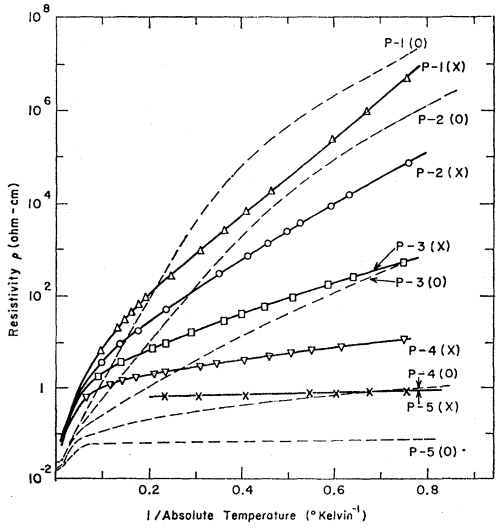

FIG. 10. Resistivity curves of the P-doped samples listed in Table I. Dashed curves represent the zero-stress resistivities, solid curves the resistivities measured at stresses of about 2×10^9 dyne cm^{-2}.

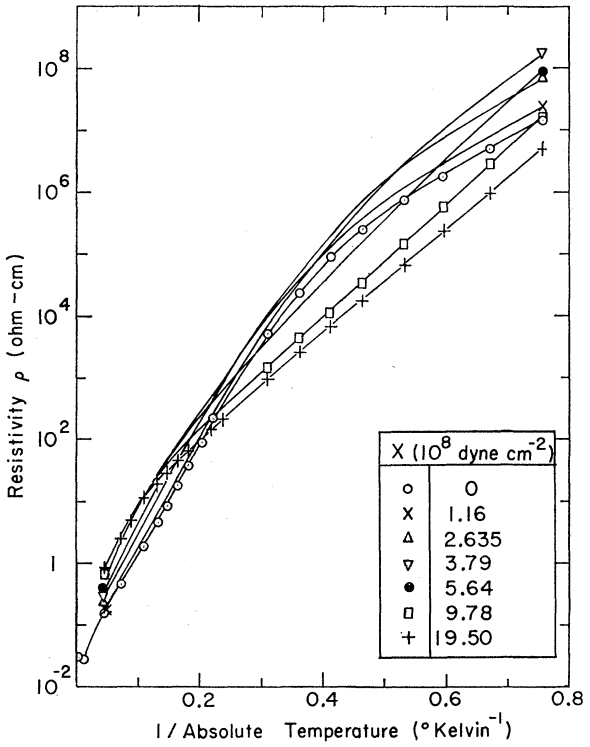

FIG. 11. Resistivity of P-1 for various stresses as a function of $1/T$. The temperature range of the activation energy ϵ_2, hardly noticeable at zero stress, increases with increasing stress.

expects a behavior of the piezoresistance somewhere in between that of Sb-doped and of As-doped germanium. That this is, in fact, the case can be seen in Fig. 9 where ρ_X/ρ_0 of sample P-1 is plotted against stress for various temperatures. One observes an appreciable increase followed by a large decrease of ρ_X/ρ_0 with stress. Figure 10 shows ρ_0 and the high-stress limit of ρ_X of all P-doped samples as a function $1/T$. The effects are less pronounced than in Sb- and As-doped germanium since the two opposing changes of the wave functions partly compensate one another.

In order to investigate in which temperature ranges the processes leading to ϵ_1, ϵ_2, and ϵ_3 are predominant, the resistivity of P-1 is plotted against $1/T$ for various stresses in Fig. 11. At the higher temperatures, ρ increases with stress as was observed in the cases of Sb- and As-doped samples in Figs. 2 and 6. A closer examination of this piezoresistance reveals that it is due to the electron transfer from the higher valleys to the lower valley in the conduction band and due to the stress-induced change of the ionization energy ϵ_1. At very low temperatures stress increases ρ, leaving the activation energy nearly unchanged. This suggests that here the ϵ_3 process dominates the conduction of P-1. Near 2.5°K small stresses hardly change the resistivity. Larger stresses, however, decrease the slope of the resistivity curve. The ϵ_2 process which is hardly noticeable in the curve of this particular sample predominates in an increasingly larger temperature range as the stress is increased. In the high-stress limit it extends from about 5°K to the lowest temperature measured.

The fact that (1) the contributions of the different conduction process to the total conduction vary with stress and (2) the conduction processes have different stress dependences, gives rise to the complicated forms of the ρ_X/ρ_0 curves in Fig. 9. There the initial increase of ρ_X/ρ_0 with stress is due to the ϵ_1 process at higher T and the ϵ_3 process at low T. The subsequent decrease of ρ_X/ρ_0 is caused by the predominance of the ϵ_2 process at higher stresses. The shapes of ρ_X/ρ_0 vs X curves change from sample to sample because the contributions of the three processes at a given temperature depend on N_D.

IV. DISCUSSION

A. General Comparison

The great differences in the piezoresistance effect of the various donors suggest that the stress-induced changes of the donor wave functions depend strongly on the size of the valley-orbit splitting. Since the overlap integral depends on the ratio d/a_H, where d is the average donor separation and a_H is an appropriate angular average of the anisotropic ground state wave function, we would like to investigate whether ϵ_2 is a function of d/a_H and how the ratios of a_H of the various donors compare with the theoretical estimates. Another possibility of comparing the sizes of a_H of the different donors at zero and at large stresses is given by the

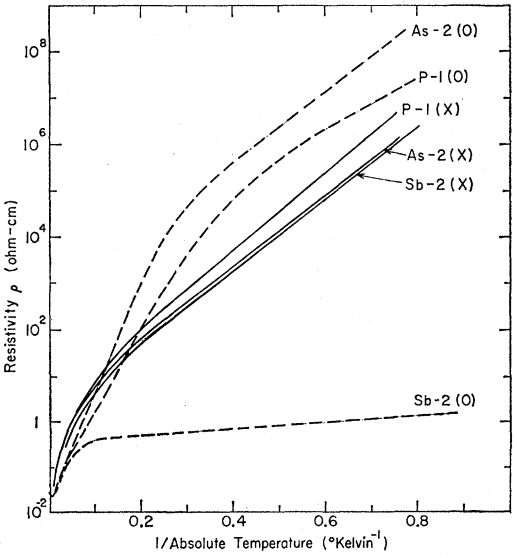

FIG. 12. Comparison of three samples which have almost identical resistivity curves at high stresses (solid curves). The dashed curves represent the corresponding resistivity curves at zero stress. It should be noted that the slopes of As-2(X) and P-1(X) below 5°K represent the conduction process of ϵ_2, which because of the large value of ϵ_2 at zero stress is hardly distinguishable from the ϵ_1 process in the cases of As-2(0) and P-1(0).

critical separation d_c which, according to Mott and Twose[4] is proportional to a_H,

$$d_c/a_H=\lambda=\text{const.} \quad (2)$$

Figure 12 compares samples containing the three donor elements, which have nearly identical resistivity curves at large stresses. In this figure the effect on ϵ_2 of the large decrease in overlap of Sb, the large increase of As, and the smaller increase in overlap of P donors is very apparent. Assuming $\epsilon_2=f(d/a_H)$ and setting $d(\text{Sb})/d(\text{As})=a_{HX}(\text{Sb})/a_{HX}(\text{As})$, where the subscript X indicates that the value is obtained at the high-stress limit, we obtain the ratios of orbit radii listed in the second row of Table II.

Figure 13 enables us to compare the critical separations d_c of the stressed and unstressed samples. The activation energy ϵ_2 is plotted against d. d_c is defined by $\epsilon_2=0$. Assuming Eq. (2), we obtain the values of the third row of Table II. These values will be compared with the theory in (II).

The ϵ_2 versus d curves of Fig. 13 can be made to nearly coincide by using d/a_H as abscissa where the a_H's have the ratios of Table II. Thus ϵ_2 and the transition to metallic conduction scale in a similar way with the size of the wave function. Unfortunately, the theories of Mott and Twose which estimate the condition for $\epsilon_2=0$ do not yield ϵ_2 as a function of d and a_H. One feels, however, that an explanation of ϵ_2 is necessary for a complete understanding of the metallic transition.

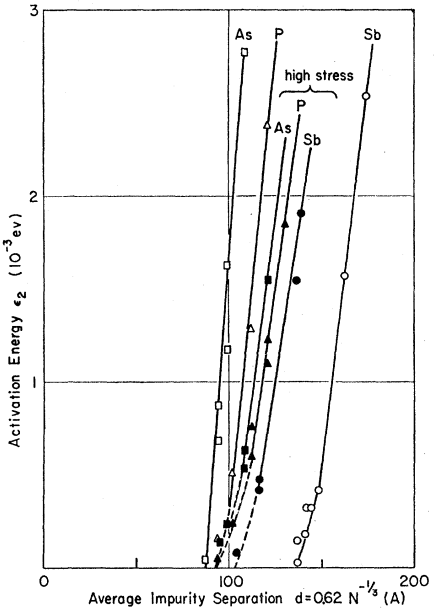

FIG. 13. Activation energy ϵ_2 as a function of the average impurity separation for the three donor elements in germanium. Zero-stress values are represented by open symbols, the high-stress values by solid symbols. The high-stress curves would move even closer together if saturation of the piezoresistance had been reached for the As- and P-doped samples. The transition to metallic conduction is defined by $\epsilon_2=0$.

B. Discussion of ϵ_2

The conduction in the transition range which exhibits the activation energy ϵ_2 still remains unexplained. One knows that it cannot be due to the presence of the higher lying threefold state because it exists also in p-type[9] and in strained n-type germanium where there are no states close to the ground state. The observed dependence of ϵ_2 on the wave-function overlap may, however, eliminate some proposed mechanisms for this conduction.

Two recent publications deal with this problem. Frood[19] proposes that the conduction takes place in the lower tail of the conduction band which includes the delocalized higher lying impurity states. He calculates the temperature- and concentration-dependent contribution of the donor levels to the dielectric constant. The dielectric catastrophe which arises by the use of the Lorentz local field in deriving the Clausius-Mossotti expression[20] is used for determining which level is delocalized. He finds that the effective ionization energy decreases with decreasing impurity separation and with increasing temperature. The predicted temperature dependence seems not to be verified by the experiments. The activation energy of Frood's model shows a distinct dependence on stress through the shift of the ground-state level and the change in polarizability of the higher excited states. This has to be studied in detail before a comparison with the experimental results can be made.

However, any model which, like the one of Frood assumes that the conduction in the transition range takes place through nonlocalized states in the tail of the conduction band, encounters difficulties in explaining the following facts. (1) The resistivity curves of this concentration range still have at higher temperatures a steeper slope which is reminiscent of the ionization energy ϵ_1. (2) The Hall curves clearly exhibit a maximum near the temperature where the ϵ_1 and ϵ_2 slopes of the resistivity curves merge. (3) At low temperatures the Hall curve show an activation energy which is less than one-half of ϵ_2. This is observed in n-type[5] as well as in p-type germanium.[9] One would have to treat the tail of the conduction band like a separate band with a mobility which decreases exponentially with $1/T$ in

TABLE II. Ratios of the effective Bohr radii.

Large stress		Zero stress	
$a_{HX}(\text{Sb})/a_{HX}(\text{As})$	$a_{HX}(\text{P})/a_{HX}(\text{As})$	$a_{H0}(\text{Sb})/a_{H0}(\text{As})$	$a_{H0}(\text{P})/a_{H0}(\text{As})$
1.10±0.02	1.07±0.02		
1.11±0.02	1.06±0.02	1.56±0.03	1.08±0.03

[19] D. G. H. Frood, Proc. Phys. Soc. (London) **75**, 185 (1960).

[20] H. Fröhlich, *Theory of Dielectrics* (Clarendon Press, Oxford, England, 1949).

order to explain these results with the concepts used in those models.

Mycielski[21] suggests that the conduction in question may be due to hopping over instead of tunneling through the Coulomb potential wall separating neighboring donors. This differs from previous models only in the way the effective height of the potential wall is calculated. The expression derived by Mycielski does not predict a stress dependence of ϵ_2 for a donor like Sb which has a very small valley-orbit splitting.

V. CONCLUSIONS

Germanium offers a unique opportunity to study the effect of the correction to the effective-mass approximations on the donor levels and on their wave functions because it has donors with greatly different valley-orbit splitting energies. For Sb the effective mass approximation is nearly correct, whereas As shows a valley-orbit splitting which is almost one-half of the effective-mass binding energy.

It is surprising that the differences in the impurity cell correction are distinctly observable even at the transition to metallic conduction where the interaction between impurities is very strong. It is interesting to investigate whether these differences affect the metallic conduction properties at even higher impurity concentrations. Preliminary experiments of the low temperature piezoresistance effect at concentrations larger than 4×10^{17} cm^{-3} show no difference between Sb- and As-doped germanium. The characteristics of Esaki diodes, however, show a difference between the donor elements.[22]

Several advantages of the use of shear strains for the investigation of impurity conduction have been mentioned and illustrated in this paper. The results obtained at large [111] compression may be better suited for a theoretical interpretation than those obtained at zero stress because of the simple, almost hydrogen-like donor level scheme produced by the compressional stress. Investigations are presently in progress of the anisotropy of the piezoresistance in the low and intermediate concentration ranges. They seem to yield further information about the nature of the observed activation energies.

The conclusions which can be drawn from the reported data concerning the strain-induced changes of the donor wave functions will be discussed in the following paper (II).

[21] J. Mycielski, Phys. Rev. **122**, 99 (1961).

[22] N. Holonyak, I. A. Lesk, R. N. Hall, J. J. Tiemann, and H. Ehrenreich, Phys. Rev. Letters **3**, 167 (1959).

PHYSICAL REVIEW VOLUME 125, NUMBER 5 MARCH 1, 1962

Effect of Stress on the Donor Wave Functions in Germanium*

H. FRITZSCHE
Department of Physics and Institute for the Study of Metals, University of Chicago, Chicago, Illinois
(Received October 19, 1961)

The effect of the corrections to the effective-mass approximation on the stress dependence of the donor wave functions has been re-examined. It is found that not only the relative valley contributions to the ground-state wave function are changed by the stress, but also the individual envelope functions $F_j(\mathbf{r})$ which originate from the j conduction-band valleys. The stress dependence of the $F_j(\mathbf{r})$ depends strongly on the value of the valley-orbit splitting of the donor. This can explain qualitatively the different behavior of the piezoresistance effect in the impurity conduction range of germanium doped with antimony, arsenic, or phosphorus. The stress dependence of the hyperfine splitting of the electron spin resonance is shown to be very insensitive to the stress-induced changes in $F_j(\mathbf{r})$ except in the limit of very large stresses.

I. INTRODUCTION

In previous calculations[1,2] of the strain-induced changes of the donor wave functions in germanium and silicon it was assumed that the only effect of strain is to admix to the ground state some of the higher-lying $1s$-like states. As an example, consider the wave functions for the donor states in germanium which can be written according to Kohn and Luttinger[3] as

$$\Psi(\mathbf{r})=\sum_{j=1}^{4}\alpha_j F_j(\mathbf{r})\varphi_j(\mathbf{r}), \tag{1}$$

where φ_j is the Bloch function at the jth conduction band minimum and $F_j(\mathbf{r})$ is the effective-mass envelope

* Work supported by the U. S. Air Force Office of Scientific Research.

[1] H. Fritzsche, Phys. Rev. **119**, 1899 (1960). An error in this paper should be pointed out. The second line of Eq. (1) should read

$$\Psi^{(2)}=\tfrac{1}{2}\sum_{j=1}^{2}[1+\epsilon_j/(4\Delta_c^2+\epsilon_j^2)^{\frac{1}{2}}]^{\frac{1}{2}}\Phi_j-\tfrac{1}{2}\sum_{j=3}^{4}[1+\epsilon_j/(4\Delta_c^2+\epsilon_j^2)^{\frac{1}{2}}]^{\frac{1}{2}}\Phi_j.$$

[2] D. K. Wilson and G. Feher, Phys. Rev. **124**, 1068 (1961). G. Feher, *Proceedings of the International Conference on Semiconductor Physics, Prague, 1960* (Czechoslovakian Academy of Sciences, Prague, 1961), p. 579.

[3] For a review on this subject see: W. Kohn in *Solid-State Physics*, edited by F. Seitz and D. Turnbull (Academic Press, Inc., New York, 1957), Vol. 5.